Research on Voltage Stability Strategy of Energy Storage Access to High Penetration Wind and Solar Power Distribution Network System with SOP (Soft Open Point)

Zhilin DING*, Wenping BU, Shuling FENG, Xing CAI, Renbo XU, Wenhao HUANG, Xiao YU, Yunfang ZHANG

Abstract: With the continuous consumption of energy, the ecology is becoming increasingly harsh. The penetration of environmentally friendly new energy, mainly symbolized via wind and solar energy, in the world new energy generation is constantly increasing, leading to changes in the modern power grid structure. Moreover, the intermittent as well as fluctuating characteristics of wind and solar power generation have enhanced its power flow imbalance. In the power network, voltage is a highly regarded indicator via measuring system stability, and therefore can be used as an indicator for measuring the stability of new power grids. This article analyzes the power flow distribution of the node system under the IEEE 33 with energy storage as well as reconstruction mode, from the perspective of the high penetration wind and solar energy storage and distribution power grid with the continuous augmentation of new energy generations. The voltage of characteristic nodes is selected as the voltage stability index, and the detecting method of the voltage fluctuation index of system nodes is established with the goal of examining the voltage fluctuation index during the continuous increase of wind and solar penetration, which provides a reference for the study of voltage stability theory and practice in high penetration wind and solar energy storage and distribution power grids.

Keywords: energy storage; high penetration; SOP; voltage stability; wind and solar power distribution network

1 INTRODUCTION

The harmonious coexistence of energy, social environment, and ecology is an important examination point related to human sustainable development. Currently, the utilization of new energy mainly focuses on energy forms such as natural gas, hydrogen, and wind and solar energy [1-4]. Due to the fact that conventional energy is mainly in the form of thermal power generation, which has planning and high stability, the utilization of new energy needs to add new evaluation elements due to the uncertainty in the interaction process with the environment. However, the low-carbon and sustainable characteristics of human social development continue to receive attention from researchers [5-10]. The penetration of new energy generation in countries around the world is increasing. Data shows that by 2030, electricity will account for about 40% of the demand for energy terminal consumption, and it will continue to climb to around 70% by 2060 [11], demonstrating that the role of new energy in human activities is becoming increasingly widespread [12].

Regarding the research on new energy, researchers around the world have different research scenarios. Iranian scholars have analyzed the positive impact of 35% new energy integration in oil rich areas on carbon emissions [13]. Chinese scholars have analyzed the stability of high penetration new energy systems in both short-term and long-term benefits. In the new power system constructed by high penetration new energy systems, the integration of energy storage systems can effectively improve the operational steadfastness of the regarded power grid [14-16].

In terms of the stability of the regarded power grid system, it is also necessary to examine the stability of the power grid under different scenarios and conditions. Small scale power grids usually use a reasonable ratio of new energy integration and thermal power to exalt the steadfastness of the power grid system [7, 17-19]. In large-scale power grid systems, it is necessary to consider the integration of energy storage links, and ameliorate the parameter stability of the new power grid through the charging and discharging effects of the energy storage system. The parameters include node voltage, line power flow, and system frequency, etc [20-26].

Energy storage technology is an effective means to solve energy consumption and improve system stability in new power grids. However, the location, capacity configuration, and access nodes of the energy storage link will manipulate the operational steadiness and economy of the new power grid [27-29]. Energy storage systems are of great significance in enhancing the flexibility of new power system [30], including enhancing system adaptability and system resilience [31], reasonable application of control strategies can provide data support for more effective operation of high penetration energy system [32-34]. With the development of energy storage technology and the rapid iteration of electric vehicle technology, the high penetration energy system under the integrated operation of energy storage and electric vehicles has also received continuous attention from researchers.

This article focuses on the stable operation of a high penetration energy system reconstruction mode. The IEEE 33 node system is connected to wind and solar generation, as well as intelligent soft open point and energy storage links to establish system flow constraints. The second-order cone algorithm is used to iteratively calculate and optimize the flow under 10% - 50% new energy generation. The voltage deviation index is established, and the fluctuation of each node is compared as a deviation index. Select the node with the highest fluctuation for analysis, compare the fluctuation index changes under different penetration of new energy generation access, and verify the rationality and effectiveness of the proposed scheme.

2 HIGH PENETRATION WIND AND SOLAR POWER DISTRIBUTION NETWORK RECONSTRUCTION MODE

With the unceasing enlargement of regarded energy generation, the stability of the bulk grid operation at the distribution end is becoming increasingly prominent. Fig. 1 shows a typical IEEE 33 node diagram of the

distribution network structure. At the nodes in the figure, new energy generations are added to characterize the energy injection status of the distribution network. During operation, structural expansion is carried out based on this to optimize the operation status of the entire distribution network system and promote better power flow operation. Set up wind power generation, photovoltaic power generation, soft open points, and energy storage links at different nodes within the system.

The specific node structure is shown in Fig. 2 and Fig. 3. During the solving procedure, the second-order cone algorithm is employed to iteratively formulate the power flow parameters, and the power flow results are obtained. As shown in Fig. 5, the 24 - hour node voltage operation diagram of the system with wind and solar penetration of 10% is shown with the energy storage link access. By analyzing the data fluctuation of each node, node 18 with the highest fluctuation is selected as the observation node to analyze the improvement of the systematic voltage parameter operation after the introduction of the energy storage link.
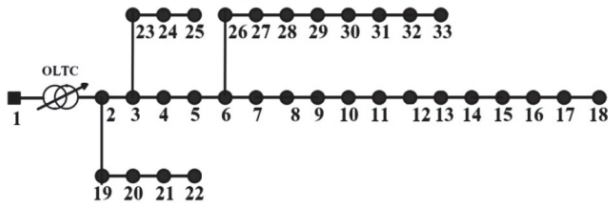

Figure 1 IEEE 33 node distribution network structure diagram

Soft Open Point (SOP), as a regarded sort power distribution gadget, is mainly installed at traditional interconnection switches. It can flexibly restrain the transmission of active power between two feeders and provide certain reactive power support. The performance of SOP is mainly supported by fully restrained power electronic gadgets. The installation of SOP can improve the flexibility and stability of power flow in the distribution network. The integration of intelligent SOP can alleviate the intermittency and uncertainty in the wind and solar high penetration energy distribution network, enhance the flow optimization between nodes. However, in the case of flow mismatch, reasonable integration of energy storage links can also enhance the flow distribution and stability of the distribution network system.
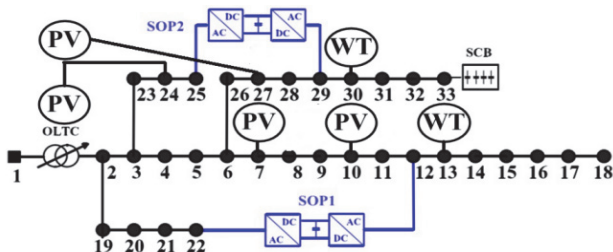

Figure 2 IEEE 33 node high penetration wind and solar reconstruction power distribution network structure

It is depicted from Fig. 2 that the IEEE 33 node high penetration distribution network reconstruction structure diagram is based on intelligent SOP and the addition of wind and solar new energy forms. Due to the increase in the penetration wind and solar new energy generations in

this structure, the fluctuation of power flow operation in the distribution network is intensified. On this basis, an energy storage link can be added to obtain the IEEE 33 node high penetration wind and solar storage reconstruction distribution system as shown in Fig. 3.
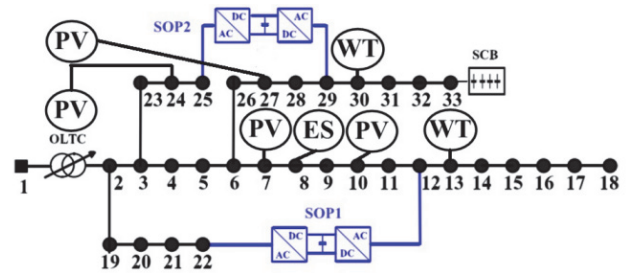

Figure 3 IEEE 33 node high penetration wind and solar energy storage reconstruction power distribution network structure

3 POWER FLOW OPTIMIZATION CONTROL METHOD FOR HIGH PENETRATION WIND AND SOLAR ENERGY STORAGE DISTRIBUTION POWER GRID NETWORK

The cone algorithm is used to describe the method of solving the problem of minimizing the linear objective function under the constraints of introducing partial order, linear equations, and inequalities into a non empty pointed convex cone. It is expressed by the cone expression:

$$x^2 + y^2 \leq C \tag{1}$$

where, x, y are variables, C is a constant term. By assigning system variables and constant terms, a second order cone expression for specific parameters can be obtained, which can enhance the rapidity of problem solving. The power flow is represented as follows:

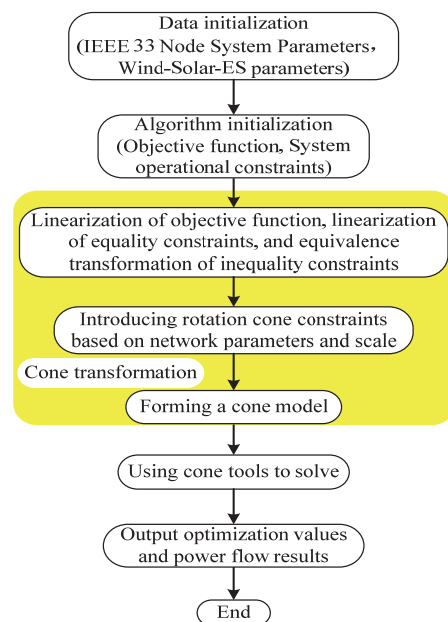$$P_i^2 + Q_i^2 \leq 2 \cdot \frac{S_{ij}}{\sqrt{2}} \cdot \frac{S_{ij}}{\sqrt{2}} \tag{2}$$

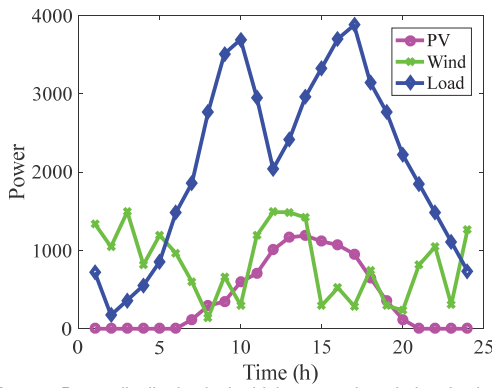**Figure 4** Optimization flowchart of second-order cone algorithm

Figure 5 Power distribution in the high penetration wind and solar power distribution network system

$$P_j^2 + Q_j^2 \leq 2 \cdot \frac{S_{ij}}{\sqrt{2}} \cdot \frac{S_{ij}}{\sqrt{2}} \tag{3}$$

where, P_i, P_j, Q_i, Q_j, S_{ij} are active power, reactive power, and apparent power at nodes, respectively, i, j correspond to different numbers of power nodes. By constraining the power expression of nodes with cone expressions and optimizing their solutions, the optimal power flow based on cone expression constraints is obtained.

The solution flowchart for second-order cone optimization under high penetration wind and solar with energy storage reconstruction based on IEEE 33 node distribution network system is shown in Fig. 4.

4 A VOLTAGE DEVIATION MODEL FOR RECONSTRUCTION MODE OF HIGH PENETRATION WIND AND SOLAR ENERGY STORAGE DISTRIBUTION POWER GRID

4.1 Voltage Deviation Index

By establishing voltage parameter observation points, the operating conditions and stability indicators of the voltage observation points under different wind and solar power supply connection ratios are tested to illustrate the improvement of system stability under the energy storage link connection. The stability indicators are described as follows:

$$S^2 = \frac{\sum \left(X - \bar{X}\right)^2}{n-1} \tag{4}$$

In the formula, S^2 is the sample variance, X is the variable, $\bar{X}$ is the sample mean, and n is the number of samples.

By substituting voltage parameters, it can be obtained that:

$$S_{Un}^2 = \frac{\sum \left(U_n - \bar{U}_n\right)^2}{n-1} \tag{5}$$

In the formula, S_{Un}^2 is the variance of node voltage samples, U_n is the variable of node voltage, $\bar{U}_n$ is the mean of node voltage samples, and n is the number of node

voltage samples, with a value of 33 in this system.

Further define the objective function:

$$f = \max[S_{Un}^2] \tag{6}$$

In the formula, f is the objective function for defining voltage demand. By establishing a solution relationship expression, the node voltage deviation index is solved. When selecting a specific observation point, the maximum deviation point can meet the demand situation, while other nodes can also meet it.

4.2 Constraints for a High Penetration Wind and Solar with Energy Storage Power Distribution Network

When setting up the energy storage system, it is necessary to consider the range of values for its state of charge S_{SOCt}:

$$S_{SOCt} = \frac{E_t}{E^{\max}} \tag{7}$$

$$0 \leq S_{SOC}^{\min} \leq S_{SOCt} \leq S_{SOC}^{\max} \leq 1 \tag{8}$$

where E_t is the actual capacity of the battery, $E^{\max}$ is maximum battery capacity, $S_{SOC}^{\min}$ and $S_{SOC}^{\max}$ are the minimum and maximum charge state values in the energy storage procedure, respectively.

The output constraints of wind and solar generation are:

$$0 \leq P_{PVt} \leq P_{PV\max} \tag{9}$$

$$0 \leq P_{Wt} \leq P_{W\max} \tag{10}$$

$$\alpha = \frac{\sum P_{PVt} + \sum P_{Wt}}{\sum P_{PVt} + \sum P_{Wt} + \sum P_{Gt}} \tag{11}$$

where, P_{PVt} is real solar generation output, $P_{PV\max}$ is maximum solar generation output, P_{Wt} is real wind generation output, $P_{Wt\max}$ is maximum wind generation output, P_{Gt} is traditional generation output, α is the proportion of wind and solar power generation to total energy generation.

The output constraint of thermal power units is:

$$P_{G\min} \leq P_{Gt} \leq P_{G\max} \tag{12}$$

where, $P_{G\min}$ is minimum output value of traditional energy generation, $P_{G\max}$ is maximum output value of traditional energy generation.

The power balance constraint equation of the wind and solar with energy storage distribution grid is:

$$\sum_{t=0}^{N_G} P_{Gt} + \sum_{t=0}^{N_{PV}} P_{PVt} + \sum_{t=0}^{N_W} P_{Wt} + P_{SOC} = P_{load} \tag{13}$$

where, P_{SOC} is the size of the stored power in the energy storage procedure, $P_{SOC} > 0$ is discharge state, $P_{SOC} < 0$ is

charging state, P_{load} is load absorption power capacity.

5 CASE ANALYSIS

The node power generation and energy storage unit settings of the reconstructed wind and solar with energy storage distribution power grid system are shown in Tab. 1. SOP1 and SOP2 are intelligent SOP, set at 12 - 22 and 25 - 29 respectively, which is used to guide the power flow between distant nodes. Wind power generations are set at nodes 13 and 30, solar power generations are set at nodes 7, 10, 24 and 27, and energy storage is set at nodes 8. The effectiveness of this method is demonstrated by comparing the monitoring points of the voltage and fluctuation indicators of the power flow operation before and after the integration of the energy storage link in the wind and solar power distribution network under the reconstruction mode.

By establishing a simulation model, the power flow operation of IEEE 33 distribution network connected to intelligent SOP under wind and solar with storage structure is calculated and solved. Firstly, the power time distribution diagram of the wind and solar distribution network system is established as shown in Fig. 5 to characterize the power characteristics of wind power generation, solar power generation, and the load. Fig. 6 shows the 24 - hour voltage operation index diagram of the system at node 33 under wind and solar integration. The penetration of wind and solar access systems in this figure is $\alpha = 10\%$. With the continuous increasing α of the system, the voltage fluctuations at system nodes intensify, which can easily cause voltage collapse and reduce system stability.

By adjusting the penetration of wind and solar power sources α after substituting 10% - 50% into the calculation and extracting data, the voltage indicators of each node are depicted by Tab. 2, as well as the voltage operation diagram of each node shown in Fig. 6. Through observation and analysis, it can be concluded that as the penetration of wind and solar power increases, the system selects voltage fluctuation that intensifies and stability decreases. The fluctuation index parameter is measured by variance to illustrate the operating voltage state of the system. In order to select specific observation points, it is necessary to further process the data in Tab. 2 and solve for the volatility.

Table 1 IEEE 33 Node High Penetration Wind and Solar with Energy Storage Distribution Grid Parameter

Designation	Arguments
Soft Open Point (SOP1, SOP2)	1:12 - 22, 2:25 - 29
Wind Generation	13(1000 kVA), 30(1000 kVA)
Solar Generation	7(500 kVA), 10(500 kVA), 24(300 kVA), 27(300 kVA)
Energy Storage System	8(100 kVA)
S_{SOC}^{min}	0.2
S_{SOC}^{max}	0.9

Table 2 Voltage operation at each node according to different penetration wind and solar generation in the High penetration wind and solar power distribution network

Node	10% High Penetration	20% High Penetration	30% High Penetration	40% High Penetration	50% High Penetration
1	12.66	12.66	12.66	12.66	12.66
2	12.66317976	12.17627962	12.18971862	12.19208253	12.19532386
3	12.68185904	12.28020005	12.36735009	12.38430164	12.40712023
4	12.70286065	12.34601511	12.49017453	12.51526692	12.5490717
5	12.72569047	12.41568315	12.61989223	12.65499795	12.70234998
6	12.77234946	12.56110713	12.88205391	12.90762657	12.95967165
7	12.77424705	12.57299119	12.9010725	12.88444402	12.90936339
8	12.79685654	12.63661729	13.02211615	13.00653352	13.04637398
9	12.83196769	12.72868911	13.19063906	13.14712792	13.18815959
10	12.86882729	12.82378493	13.36481161	13.2970947	13.34406829
11	12.87615556	12.83941636	13.39371023	13.32435048	13.37385671
12	12.89042349	12.86950513	13.44908397	13.37674149	13.43125258
13	12.95282269	13.04476052	13.72296539	13.59115115	13.63236747
14	12.94782665	13.03979978	13.71824985	13.50277447	13.48574944
15	12.94471866	13.03671436	13.71531687	13.42737185	13.35984428
16	12.94170965	13.03372683	13.71247719	13.34196252	13.21690781
17	12.9372502	13.02929895	13.70826854	13.23688284	13.04112474
18	12.93591488	13.02797307	13.70700833	13.23557768	13.03980006
19	12.66279824	12.18311321	12.19647017	12.19864728	12.20188844
20	12.66238879	12.24816733	12.26052855	12.26118677	12.26449724
21	12.66296177	12.26782345	12.28020001	12.28020021	12.28344287
22	12.66540358	12.30460884	12.31728937	12.31591002	12.3189509
23	12.67332752	12.29519105	12.37921613	12.40220219	12.43332699
24	12.65737517	12.32671887	12.40280296	12.43830176	12.48700544
25	12.6494344	12.35758105	12.41722481	12.45649197	12.51403332
26	12.77953221	12.57896814	12.91471828	12.94822116	13.00642746
27	12.78990648	12.60430869	12.96084713	13.00557963	13.07259274
28	12.82798856	12.68452136	13.09558221	13.15471338	13.22658013
29	12.85798162	12.74676907	13.20073694	13.27310061	13.35163561
30	12.87888352	12.80668148	13.29587404	13.38403425	13.47481779
31	12.87860735	12.80189853	13.28692074	13.31588362	13.33957756
32	12.87994496	12.80154969	13.28495065	13.29299998	13.293
33	12.88425295	12.80340054	13.28433992	13.27842513	13.26258789

By solving the changes in the above voltage indicators and establishing the fluctuation monitoring points, the data shown in Tab. 3 can be obtained. The observation data shows that selecting node 18 as its fluctuation monitoring indicator is more reasonable to evaluate the impact of energy storage on the system voltage indicators under high proportion energy operation.
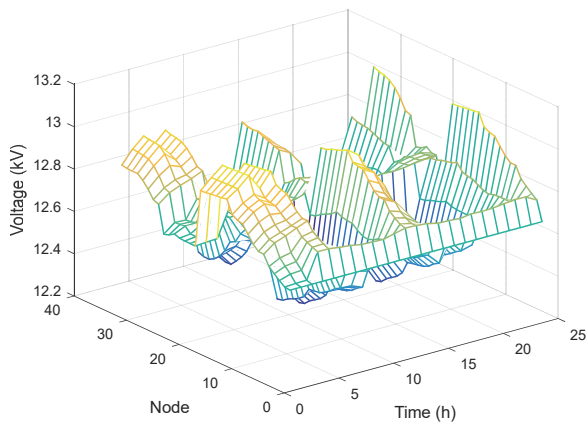
represents the discharge status, and when it is minus than 0, it represents the charging status.

Figure 6 Node voltage waveform diagram in the high penetration wind and solar power distribution network system
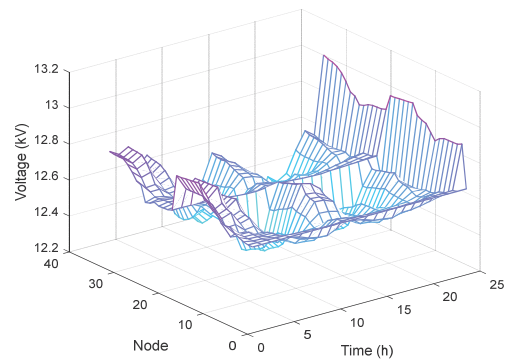

Figure 7 Node voltage waveform diagram in the high wind and solar penetration with energy storage distribution power grid system

By calculating the 10% - 50% wind solar power ratio through the high penetration energy system connected to the energy storage link, the voltage operation index data of each node is obtained as shown in Tab. 4, and the voltage deviation index data is shown in Tab. 5.

By extracting the node voltage data of the high wind and solar penetration with energy storage distribution power grid system, a three-dimensional voltage operation diagram of the 10% high wind and solar penetration with energy storage distribution power grid can be obtained in Fig. 7. The charging and discharging status of the energy storage link in this operation mode is shown in Fig. 8. When the energy storage link data is larger than 0, it
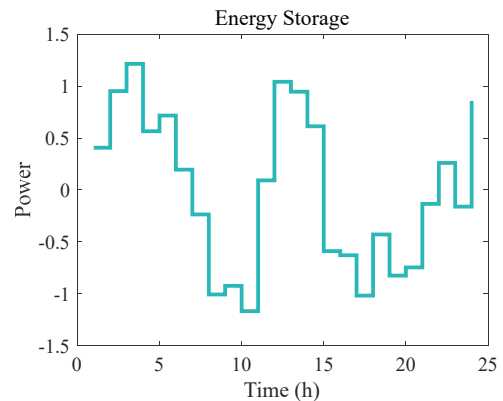

Figure 8 Energy storage link power flow in the high penetration wind and solar with energy storage and distribution power grid system at different times

Table 3 Voltage deviation for nodes with different wind to solar penetration in the high penetration wind and solar distribution network

Node	10% High Penetration	20% High Penetration	30% High Penetration	40% High Penetration	50% High Penetration
1	0	0	0	0	0
2	0.001410902	0.010501633	0.012941551	0.022885147	0.062778568
3	0.002119349	0.003989675	0.004853855	0.017276537	0.051974895
4	0.004230688	0.00267214	0.003753585	0.016441202	0.046837914
5	0.007516932	0.002861215	0.006029048	0.018168386	0.044109585
6	0.019035274	0.008247432	0.020227368	0.025354522	0.038646973
7	0.021006818	0.008937263	0.021226894	0.02101912	0.03146078
8	0.026326636	0.013262814	0.032560823	0.026615961	0.032202816
9	0.033348657	0.019963711	0.050939032	0.032673364	0.031279333
10	0.040806615	0.028336963	0.074606061	0.042150942	0.034870302
11	0.042393729	0.030127251	0.079084143	0.044181513	0.034475793
12	0.045342224	0.033658071	0.088098806	0.048527713	0.034339926
13	0.064491154	0.059796886	0.131869485	0.066250215	0.032704088
14	0.067993076	0.062335597	0.13172558	0.060633423	0.026184102
15	0.070247484	0.063987868	0.131081194	0.059068648	0.027326339
16	0.072484975	0.065640499	0.130179933	0.061314521	0.036391594
17	0.075901156	0.068186278	0.129719418	0.070294043	0.058619236
18	0.076946354	0.068970315	0.130501571	0.070591764	0.058391169
19	0.001328889	0.009938782	0.012431688	0.022654787	0.062464698
20	0.001286624	0.006495194	0.009081291	0.021270469	0.060378293
21	0.001420463	0.005878282	0.008294247	0.021009982	0.059941516
22	0.001693782	0.005119224	0.007117641	0.020681935	0.059343716
23	0.002980649	0.003321018	0.004248163	0.017027079	0.052073134
24	0.005384287	0.003288618	0.003615333	0.016969796	0.053029977
25	0.0072396	0.004538514	0.00319821	0.015926842	0.051228287
26	0.020900287	0.009388197	0.022933937	0.028162742	0.039802398
27	0.023543023	0.011102586	0.027105026	0.032629149	0.042003872
28	0.035961298	0.019277333	0.04170968	0.048253506	0.041900315
29	0.046774745	0.027397803	0.057330621	0.067005605	0.049214126
30	0.05497955	0.036297456	0.072464308	0.084217435	0.059528805
31	0.059980892	0.039610161	0.073377516	0.078560477	0.043056072
32	0.060888371	0.040176632	0.07299759	0.076199184	0.038441481
33	0.060524561	0.039812232	0.071216287	0.074025521	0.035638089

Table 4 Voltage operation at each node according to different penetration of wind and solar generation with energy storage in the High penetration wind and solar power distribution network

Node	10% High Penetration	20% High Penetration	30% High Penetration	40% High Penetration	50% High Penetration
1	12.66	12.66	12.66	12.66	12.66
2	12.66017078	12.29880036	12.18734353	12.19076887	12.19509046
3	12.66543545	12.38395112	12.35182783	12.37555394	12.40529905
4	12.67647593	12.4363602	12.46440031	12.50103893	12.54593443
5	12.68892534	12.49203811	12.58333961	12.63483186	12.69744837
6	12.71260267	12.6047498	12.82229556	12.87685615	12.95496497
7	12.70817825	12.60751436	12.83579657	12.85182915	12.91196431
8	12.71142282	12.64718525	12.93506216	12.95586667	13.03979999
9	12.75070317	12.73582838	13.10453919	13.10441938	13.2067031
10	12.79185361	12.82757829	13.27972665	13.26238036	13.38746126
11	12.80015745	12.8429788	13.30879535	13.2907795	13.42067453
12	12.81628605	12.87263114	13.36449571	13.34534173	13.48454798
13	12.87903582	13.0478445	13.64001938	13.57158037	13.72159921
14	12.8740101	13.04288481	13.63527507	13.48875241	13.59416098
15	12.87088379	13.03979998	13.63232412	13.41816082	13.48488266
16	12.86785725	13.03681316	13.62946706	13.33823307	13.36087993
17	12.86337228	13.03238634	13.62523278	13.23987043	13.20842029
18	12.86202929	13.03106077	13.62396489	13.23856564	13.20711239
19	12.6588783	12.30384951	12.19428245	12.19743734	12.20160382
20	12.65013355	12.35339809	12.25995905	12.26086136	12.26376361
21	12.64841121	12.36769808	12.28019996	12.2802	12.28255952
22	12.64685301	12.39408165	12.31840282	12.3165564	12.31778127
23	12.65689272	12.39801801	12.36423455	12.39295921	12.43099614
24	12.64091934	12.42741122	12.38902297	12.42794741	12.48352406
25	12.6329681	12.45617786	12.40461838	12.44502991	12.50941305
26	12.7198179	12.62207521	12.85510545	12.91869011	13.00191117
27	12.73023871	12.64666721	12.90143996	12.97777921	13.06834298
28	12.76849345	12.72258129	13.0369411	13.13500975	13.22349055
29	12.79862392	12.78162612	13.14268917	13.25947641	13.34942946
30	12.81962164	12.8413773	13.23823928	13.37341813	13.47310326
31	12.81934331	12.83660773	13.22924685	13.3131125	13.33913013
32	12.82068691	12.83626004	13.22726839	13.293	13.293
33	12.82501479	12.83810588	13.22665502	13.2802762	13.26288714

Table 5 Voltage deviation for nodes with different wind to solar penetration in the high penetration wind and solar with energy storage distribution network

Node	10% High Penetration	20% High Penetration	30% High Penetration	40% High Penetration	50% High Penetration
1	0	0	0	0	0
2	0.002583119	0.001570748	0.000112334	0.017994827	0.069389615
3	0.003849845	0.001025374	0.000279303	0.014736464	0.055402402
4	0.004408785	0.000979926	0.000621169	0.013369145	0.046942405
5	0.004938496	0.000974556	0.001245202	0.012714939	0.039395465
6	0.006608934	0.001156681	0.003544725	0.013040332	0.026450997
7	0.006408182	0.00106792	0.005392271	0.016336107	0.027855085
8	0.004803515	0.001920387	0.019538064	0.041828877	0.041719726
9	0.007494613	0.001391556	0.008031056	0.018848847	0.021157296
10	0.011588893	0.004145631	0.004492471	0.008179779	0.015569293
11	0.01262326	0.005095608	0.004691013	0.006760861	0.01428783
12	0.0146616	0.00719357	0.005813097	0.005206159	0.013096749
13	0.02563877	0.021778942	0.01970263	0.013035377	0.023835735
14	0.027877743	0.023520706	0.021078281	0.014135252	0.025865713
15	0.029345244	0.024675376	0.022000676	0.015431286	0.029024984
16	0.03082033	0.025845053	0.022942243	0.01731956	0.034162425
17	0.033105285	0.027672706	0.024425821	0.020301529	0.042260651
18	0.033811828	0.028241347	0.024890176	0.020385926	0.041812245
19	0.002662092	0.001483796	0.000112179	0.01785767	0.069054612
20	0.003432397	0.001181837	0.000361086	0.017127617	0.066803116
21	0.003632531	0.001187509	0.000464545	0.017017037	0.06633408
22	0.003827376	0.001222372	0.000580346	0.016874141	0.065704299
23	0.004941245	0.001206929	0.000340574	0.014202713	0.054580671
24	0.00773985	0.002465116	0.000742267	0.013539063	0.053738661
25	0.009820537	0.004005638	0.001025979	0.01238716	0.051392427
26	0.007557897	0.001475348	0.002761629	0.010567653	0.023532407
27	0.008982731	0.002128824	0.002258888	0.00807871	0.020296464
28	0.017013627	0.007590951	0.006610996	0.006160018	0.011229062
29	0.024764282	0.014363448	0.016393193	0.015515111	0.012817613
30	0.030610116	0.021075274	0.025363353	0.025850294	0.018114366
31	0.034410706	0.023971927	0.027085698	0.027857707	0.012013252
32	0.035097081	0.024494686	0.027169364	0.028217937	0.010338109
33	0.034787583	0.024246034	0.026365979	0.028205305	0.009332052

By comparing the voltage operation diagrams of high penetration wind and solar with energy storage integration, the voltage distribution at node 18 with high voltage fluctuation is taken as the inspection point. By monitoring its voltage waveform and fluctuation index data, the voltage operation of node 18 before and after energy

storage integration is shown in Fig. 9 and Fig. 10, and the fluctuation degree index of nodes is shown in Fig. 11 and Fig. 12; it can be seen that the fluctuation index at node 18 has been improved after the energy storage is connected, and the system stability has been improved.
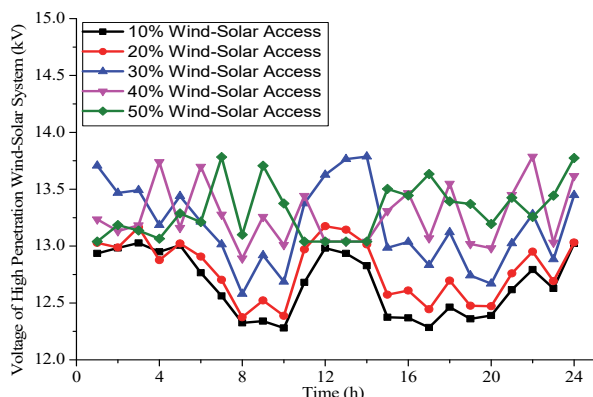

Figure 9 Voltage operation diagram of node 18 under high penetration wind and solar integration

This characteristic is particularly prominent in the stability improvement effect reflected by the wind solar power penetration of 40% - 50%. The data in Tab. 3 and Tab. 5 have decreased from 0.070591764 and 0.058391169 to 0.020385926 and 0.041812245, indicating a good improvement effect. If analyzed from a structural perspective again, under the dual effects of intelligent soft switching and energy storage before and after reconstruction, the power flow of the IEEE 33 node distribution network system has better voltage stability.
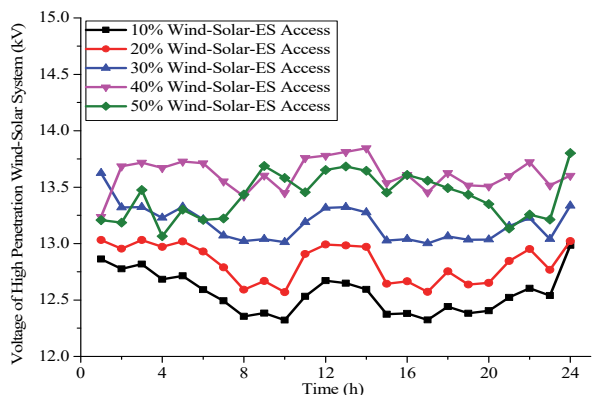

Figure 10 Voltage operation diagram of node 18 under high penetration wind and solar integration with energy storage
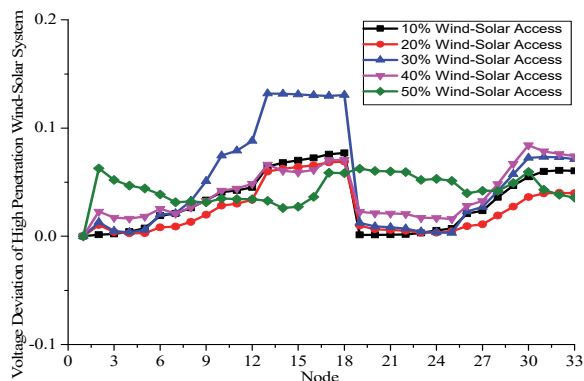

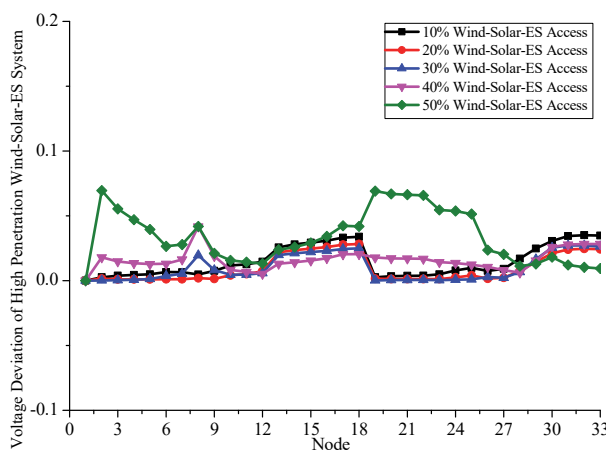**Figure 11** Voltage deviation of various nodes in high penetration wind and solar integration structure

Figure 12 Voltage deviation of various nodes in the high penetration wind and solar integration with energy storage structure

6 CONCLUSION

This article is based on the monitoring of voltage deviation improvement under the reconstruction of energy storage structure in a high penetration wind and solar power distribution network system. By adding intelligent soft point and energy storage links at nodes on the existing high penetration wind and solar power distribution network structure, a voltage deviation evaluation index is established. The second-order cone algorithm is used to obtain the voltage deviation characteristics at various times and nodes during the power flow operation process. Compare and extract the data of the maximum voltage fluctuation point as the basis for voltage deviation. The comparative analysis of data shows that under the integration of intelligent soft point and energy storage structures, the voltage deviation of the high penetration new energy operation mode in the IEEE 33 node distribution network is effectively improved through second-order cone optimization and observation at node 18.

7 REFERENCES

[1] Berrill, P., Arvesen, A., Scholz, Y., Hans, C. G., & Edgar, G. H. (2016). Environmental impacts of high penetration renewable energy scenarios for Europe. *Environmental Research Letters, 11*(2016), 14012. https://doi.org/10.1088/1748-9326/11/1/014012

[2] Sheng, C., Jingchun, Z., Zhinong, W., et al. (2023). Energy Transition Oriented Planning and Operation of Electricity-Gas-Hydrogen Integrated Energy System. *Automation of Electric Power Systems, 47*(19), 16-30.

[3] Feng, L., Jie, D., Caiqi, Z., et al. (2023). Discussion on Key Technologies of Large-scale Grid-connected Operation of Distributed Photovoltaic under the New-type Power System. *Power System Technol*ogy, *2023*, 1-10.

[4] Shweta, R., Sivagnanam, S., & Kumar, K. A. (2023). IoT-based Deep Learning Neural Network (DLNN) algorithm for voltage stability control and monitoring of solar power generation. *Advances in Production Engineering & Management, 18*(4), 447-461. https://doi.org/10.14743/apem2023.4.484

[5] Impram, S., Nese, S. V., & Oral, B. (2020). Challenges of renewable energy penetration on power system flexibility A survey. *Energy Strategy Reviews, 31*(2020), 100539. https://doi.org/10.1016/j.esr.2020.100539

[6] Matsuo, Y., Endo, S., Nagatomi, Y., Yoshiaki, S., Ryoichi, K., & Yasumasa, F. (2020). Investigating the economics of the power sector under high penetration of variable renewable energies. *Applied Energy, 267*(2020), 113956. https://doi.org/10.1016/j.apenergy.2019.113956

[7] Shair, J., Li, H., Hu, J., & Xie, X. (2021). Power system stability issues, classifications and research prospects in the context of high-penetration of renewables and power electronics. *Renewable and Sustainable Energy Reviews, 145*(2021), 111111. https://doi.org/10.1016/j.rser.2021.111111

[8] Yu, L., Sun, H., Xu, S., Bing, Z., & Jian, Z. (2022). A Critical System Strength Evaluation of a Power System with High Penetration of Renewable Energy Generations. *CSEE Journal of Power and Energy Systems, 8*(3), 710-720. https://doi.org/10.17775/CSEEJPES.2021.03020

[9] Collados, R. C., Cheah, M. M., Prieto, A. E., & Oriol, G. B. (2022). Stability and operation limits of power systems with high penetration of power electronics. *International Journal of Electrical Power and Energy Systems, 138*(2022), 107728. https://doi.org/10.1016/j.ijepes.2021.107728

[10] Medina, C., Ana, C. R. M., & González, G. (2022). Transmission Grids to Foster High Penetration of Large-Scale Variable Renewable Energy Sources -A Review of Challenges, Problems, and Solutions. *International Journal of Renewable Energy Research, 12*(1), 146-169.

[11] Zhigang, Z. & Chongqing, K. (2022). Challenges and Prospects for Constructing the New-type Power System Towards a Carbon Neutrality Future. *Proceedings of the CSEE, 42*(8), 2806-2818.

[12] Yue, Q., Shuai, L., Hai, L., et al. (2022). Flexibility of Integrated Energy System: Basic Connotation, Mathematical Model and Research Framework. *Automation of Electric Power Systems, 46*(17), 16-43.

[13] Pourarshad, M., Noorollahi, Y., Atabi, F., & Panahi, M. (2020). Sustainable energy system modelling with a high renewable energy penetration rate for rich oil regions. *International Journal of Sustainable Energy, 2020*, 1-20. https://doi.org/10.1080/14786451.2020.1821684

[14] Chen, S., Liu, P., & Li, Z. (2020). Low carbon transition pathway of power sector with high penetration of renewable energy. *Renewable and Sustainable Energy Reviews, 130*(2020), 109985. https://doi.org/10.1016/j.rser.2020.109985

[15] Xu, B., Zhang, G., Li, K., et al. (2022). Reactive power optimization of a distribution network with high-penetration of wind and solar renewable energy and electric vehicles. *Protection and Control of Modern Power Systems, 7*(1), 51.

[16] Zhaohui, Q., Wei, L., Tao, J., et al. (2023). Adaptability Research of Frequency Correction Control Strategy For High Proportion New Energy Grid. *Power System Technology, 2023*, 1-8.

[17] Alam, M. S., Al, I. F. S., Salem, A., & Mohammad, A. A. (2020). High-Level Penetration of Renewable Energy Sources Into Grid Utility Challenges and Solutions. *IEEE Access, 8*(2020), 190277-190299. https://doi.org/10.1109/ACCESS.2020.3031481

[18] Adetokun, B. B., Muriithi, C. M., & Ojo, J. O. (2020). Voltage stability assessment and enhancement of power grid with increasing wind energy penetration. *International Journal of Electrical Power and Energy Systems, 120*(2020), 105988. https://doi.org/10.1016/j.ijepes.2020.105988

[19] Dalala, Z., Al, O. M., Al, A. M., Mathhar, B., Yaqoub, Al K., & Malek, A. (2022). Increased renewable energy penetration in national electrical grids constraints and solutions. *Energy, 246*(2022), 123361. https://doi.org/10.1016/j.energy.2022.123361

[20] Zhang, C., Cheng, H., Liu, L., Heng, Z., Xiaohu, Z., Gang, L. (2020). Coordination planning of wind farm, energy storage and transmission network with high-penetration renewable energy. *International Journal of Electrical Power and Energy Systems, 120*(2020), 105944. https://doi.org/10.1016/j.ijepes.2020.105944

[21] Yosef, G. B., Navon, A., Poliak, O., et al. (2021). Frequency stability of the Israeli power grid with high penetration of renewable sources and energy storage systems. *Energy Reports, 7*(2021), 6148-6161. https://doi.org/10.1016/j.egyr.2021.09.057

[22] Zhang, C., Liu, L., Cheng, H., et al. (2021). Frequency-constrained Co-planning of Generation and Energy Storage with High-penetration Renewable Energy. *Journal of Modern Power Systems and Clean Energy, 9*(4), 760-775. https://doi.org/10.35833/MPCE.2020.000743

[23] Lu, H., Chunya, Y., Chen, D., et al. (2024). Transient voltage operational risk of a high-proportion new energy sending system. *Power System Protection and Control, 52*(1), 23-34.

[24] Qiangqiang, W., Liangzhong, Y., Jian, X., et al. (2024). S-MCMC Based Equivalent Inertia Probability Evaluation for Power Systems With High Proportional Renewable Energy. *Power System Technology, 48*(1), 140-149.

[25] Chang, Y., Dan, L., Xinyi, Y., et al. (2023). Optimal Operation Strategy of High Proportion New Energy Power System Based on Minimum Inertia Evaluation. *Power System Technology, 47*(2), 502-509.

[26] Bing, Z., Shiyun, X., Tiankai, L., et al. (2023). Benchmark for AC-DC Hybrid System with High Penetration of Renewables (3): Voltage Stability Benchmark CSEE-VS. *Proceedings of the CSEE, 2023*, 1-13.

[27] Weiqing, S., Jing, L., & Jie, Z. (2021). Energy storage capacity allocation and influence factor analysis of a power system with a high proportion of wind power. *Power System Protection and Control, 49*(15), 9-18.

[28] Zhiyong, S., Caixia, W., & Jing, H. (2022). A price formation mechanism and cost diversion optimization method for designing an independently new energy-storing power station. *Energy Storage Science and Technology, 11*(12), 4067-4076.

[29] Xiaorong, X., Ningjia, M., Wei, L., et al. (2023). Functions of Energy Storage in Renewable Energy Dominated Power Systems: Review and Prospect. *Proceedings of the CSEE, 43*(1), 158-168.

[30] Zongxiang, L., Yisha, L., Ying, Q., et al. (2022). Flexibility Supply-Demand Balance in Power System with Ultra-high Proportion of Renewable Energy. *Automation and Electric Power Systems, 46*(16), 3-16.

[31] Guangchun, R., Yiliu, H., Zhenfei, T., et al. (2023). Review of Hybrid Data-Driven and Physics-Based Modeling for the Operation of New-Generation Power Systems. *Proceedings of the CSEE, 29*(00), 1-20.

[32] Lin, Y., Kaifeng, W., Yening, L., et al. (2023). Review of Frequency Characteristics Analysis and Battery Energy Storage Frequency Regulation Control Strategies in Power System Under Low Inertia Level. *Power System Technology, 47*(2), 446-462.

[33] Gengfeng, L., Shaohua, S., Zhaohong, B., et al. (2023). Review on Optimal Configuration and Flexible Scheduling Research of Energy Storage for Resilience Improvement of New Power System. *High Voltage Engineering, 49*(10), 4084-4095.

[34] Huachun, H., Qiang, L., & Zhenhua, L. (2023). A

Coordinated Frequency Modulation Method Based on Adaptive Selection of Droop Coefficient for Multiple Energy Storage Combined Voltage Sources. *Power System and Clean Energy, 39*(3), 116-125.

Contact information:

Zhilin DING
(Corresponding author)
Nanchang Institute of Science & Technology,
School of Information and Artificial Intelligence,
Jiangxi, Nanchang, 330108, China
E-mail: gold_my_fency@163.com

Wenping BU
Nanchang Institute of Science & Technology,
School of Information and Artificial Intelligence,
Jiangxi, Nanchang, 330108, China

Shuling FENG
Nanchang Institute of Science & Technology,
School of Information and Artificial Intelligence,
Jiangxi, Nanchang, 330108, China

Xing CAI
Nanchang Institute of Science & Technology,
School of Information and Artificial Intelligence,
Jiangxi, Nanchang, 330108, China

Renbo XU
Nanchang Institute of Science & Technology,
School of Information and Artificial Intelligence,
Jiangxi, Nanchang, 330108, China

Wenhao HUANG
Nanchang Institute of Science & Technology,
School of Information and Artificial Intelligence,
Jiangxi, Nanchang, 330108, China

Xiao YU
Nanchang Institute of Science & Technology
School of Information and Artificial Intelligence,
Jiangxi, Nanchang, 330108, China

Yunfang ZHANG
Nanchang Institute of Science & Technology,
School of Information and Artificial Intelligence,
Jiangxi, Nanchang, 330108, China